Observations of the Nocturnal Boundary Layer associated with the West African Monsoon

Caroline L. Bain *

Department of Earth System Science, University of California, Irvine, USA

Douglas J. Parker

School of Earth and Environment, University of Leeds, Leeds, UK

Christopher M. Taylor

Centre for Ecology and Hydrology, Wallingford, UK

Laurent Kergoat

CESBIO, Toulouse, France

Francoise Guichard

CNRM-GAME, Toulouse, France

* *Corresponding author address:* Caroline Bain, Department of Earth System Science, University of California, Irvine, CA 92697. USA

E-mail: cbain@uci.edu

ABSTRACT

A set of night time tethered balloon and kite measurements from the central Sahel (15.2°N, 1.3°W) in August 2005 were acquired and analyzed. A composite of all nights' data was produced using boundary layer height to normalize measured altitudes. The observations showed some typical characteristics of nocturnal boundary layer development, notably a strong inversion after sunset and the formation of a low-level nocturnal jet later in the night. On most nights, the sampled jet did not change direction significantly during the night.

The boundary layer thermodynamic structure displayed some variations from one night to the next. This was investigated using two contrasting case studies from the period. In one of these case studies (18 August 2005), the low level wind direction changed significantly during the night. This change was captured well by two large scale models, suggesting that the large scale dynamics had a significant impact on boundary layer winds on this night. For both case studies, the models tended to underestimate near-surface wind speeds during the night; a feature which may lead to an underestimation of moisture flux northwards by models.

1. Introduction

The West African monsoon is caused by the northwards shift in the inter-tropical front during northern hemisphere summer months. The shift is a result of increased heating over the Sahara generating a heat low, simultaneous with cooling of the sea surface temperatures over the Gulf of Guinea, creating a pressure gradient between the cooler Atlantic coast of West Africa and the north (Sultan and Janicot 2003). The seasonal time scale of the monsoon

is important for annual rainfall amounts, and the daily weather is influenced by the diurnal cycle of convection which is reliant on monsoon and African Easterly Wave (AEW) processes for moisture supply.

Observation and model studies have documented the large scale dynamics of the West African monsoon, the formation of the African Easterly Jet and AEWs (e.g. Burpee 1972; Thorncroft and Hoskins 1994; Berry and Thorncroft 2005). Despite these efforts there are continuing issues associated with the modeling of the monsoon and the relationship between the monsoon and AEWs is still relatively unexplored. The consequence of this knowledge deficit is an inaccurate representation of West African rainfall by numerical models, leading to poor forecast ability (Washington et al. 2006b).

Moisture transport to northern regions of West Africa is characterised by the diurnal cycle of monsoon winds. This was summerized in Parker et al. (2005a): during the day convection in the boundary layer imposes a drag on horizontal winds, but at night turbulence decreases due to surface cooling allowing the northwards penetration of the monsoon. Hence, the strongest wind speeds associated with the monsoon inflow are instigated during night time (Dolman et al. 1997), and around the time of monsoon onset the nocturnal low level flow is primarily responsible for moisture transport to the northern Sahel (confirmed in the humidity budget in Lothon et al. 2008). This emphasizes the importance of understanding the nocturnal boundary layer (NBL) and gives motivation for observation studies. Improved understanding of NBL processes could also impact on the prediction of convection: for example, Vilà-Guerau de Arellano (2007) found that changes in nocturnal boundary layer profiles had an impact on the generation of convection during the day.

The monsoon moist inflow is known to slope vertically downwards with latitude and is

driven primarily by pressure gradients (Parker et al. 2005b). In the Sahel region (13-17°N), the monsoon inflow is confined to a 1-2 km layer near the surface, existing solely in the boundary layer (Parker et al. 2005b). The nocturnal jet at 15°N reverses direction between wet and dry seasons (Guichard et al. 2009) and is driven primarily by pressure gradients, not sloping terrain. This latitude is therefore an ideal location for studying the NBL in the context of larger scale monsoon processes. However, boundary layer observations in the Sahel region have been limited. Poor communication facilities, socio-economic difficulties and environmental harshness have resulted in few meteorological observations available outside of main cities. Few night time observations exist, apart from midnight radiosoundings.

Previous observation campaigns have highlighted the role of the diurnal cycle on the West African weather. Even early studies such as that of Hamilton and Archbold (1945) included references to the diurnal cycle of winds and convection. McGarry and Reed (1978) looked at the diurnal cycle using satellite and rainfall data from the GATE field campaign and Culf (1992) used station and radiosonde data to look at the daytime boundary layer during the SEBEX campaign (Wallace et al. 1990). More recently, the diurnal variations in the low-level circulation during the Harmattan dry season were investigated in the BoDEx field campaign in Chad (Washington et al. 2006a; Washington and Todd 2005). The speed of the low-level wind was found to peak during the night and be weakest during the day, in agreement with studies from other areas of the globe (for example Mahrt et al. 1979). Subsequent studies of the NBL (Abdou et al. 2009; Lothon et al. 2008; Pospichal et al. 2009) have been conducted as part of the African Monsoon Multidisciplinary Analysis (AMMA) field campaign (Redelsperger et al. 2007; Lebel et al. 2009). These papers have provided valuable insights into NBL mechanisms, but the observations are sparse in number and there

has not been a set of measurements from the northern Sahel region during the monsoon.

This paper presents a unique new observational dataset of the NBL in the Sahel. Tethered balloon soundings were conducted in August 2005 in Agoufou (15.2°N, 1.3°W), Mali, as part of the AMMA field campaign. The balloon recorded temperature, humidity, wind speed and direction simultaneously. The Sahelian location of Agoufou is ideal for studying the diurnal cycle in monsoon winds.

The key objective of the study is to provide an overview of nocturnal boundary layer conditions in this rarely visited region. In addition we compare the observations to output from global forecast models.

The experiment results are presented in two ways: mean evolution of profiles is shown and the night-to-night variability is explored with more detailed analysis of two nights. The field work is described in section 2 and general results are given in section 3. Section 4 looks at the variability in the two case study nights. Section 5 discusses the results and the impact that larger scale meteorology has on the local boundary layer in the Sahel, while section 6 contains the final summary.

2. Overview of experiments

a. Data collection method

The experiments that took place in August 2005 used a tethered balloon to profile the Sahelian boundary layer up to 200 m. A parafoil kite was used in high winds (approximately 10 ms^{-1}) as such conditions were not suitable for balloon flight. Soundings were made

approximately every hour from sunset to dawn. The measurements were taken by a Vaisala TS-5A-SP Tethersonde, sampling every 1.5 seconds giving pressure, temperature and relative humidity. The wind speed and direction were determined by a mounted anemometer on the sonde, and standard tailfins were added to give balance and align the sonde with the wind to monitor wind direction. The balloon was a Vaisala Tethered Balloon TTB Series, filled with helium, with dimensions 3.8 m in length, 1.85 m in diameter.

The balloon was stopped every 10 m for 30 seconds during ascent/descent up to 100 m and every 20 m above that height. This was to reduce the influence of the movement of the balloon from the wind readings; thus only the readings within these stops are included in the results for wind. The stop duration of 30 seconds was decided upon as a compromise between allowing sufficient time for the balloon to settle, and getting as many measurements in the night as possible. The temperature and humidity readings were taken continually as the movement of the balloon has minimal effect on these. On average, each profile took approximately 20 minutes to complete including stops. In total 12 nights were sampled; the number of readings on each night was dependent on weather conditions.

The field site was located at 15.2°N, 1.3°W in a relatively flat region of grassland and small trees; the nearest farmed area was a kilometer to the north at the Agoufou village. Full details of the site are given in Mougin et al. (2009). The nearest significant orography was the table-like structure of Mount Hombori, reaching 848 m above local ground level, located approximately 30 km to the west and surrounded by plains. The terrain of the field site was slightly rolling, with maximum hill elevations of 10 m. The location was very close to the transition between seasonal grassland and desert.

Information from Centre for Ecology and Hydrology (CEH) and CESBIO automatic

weather stations were consulted. One CEH station was at Agoufou near the balloon site. The second CEH station was at Edgerit (15.5°N, 1.4°W), much less vegetated than Agoufou with mainly gravelly red soil and few shrubs. The Vaisala WXT510 Weather Transmitter instrument was used to gain temperature and wind information. The stations were installed by the Centre for Ecology and Hydrology (CEH), assisted by CESBIO/IRD scientists from Bamako. Data from the CESBIO automatic weather station at Bamba (17.1°N, 1.4°W, 95% sand soil, sparse vegetation) was used as the CEH station was not functioning at this time. A full list of instrumentation and specifications can be found at http://amma.mediasfrance.org/implementation/instruments.

b. Numerical models

Global forecast models are able to accurately simulate large scale dynamical motions days in advance but are less able to capture small scale variability such as convergence and convection. This is partly because of lack of resolution, lack of observations to initialize the model, the model surface description, and the limits of soil, turbulent convection and near-surface data assimilation and parameterizations.

Due to their good representation of large scale flow, models can be used to some extent to ascertain whether the balloon measurements are representative of a larger area, creating a context for the observations. It is also useful to compare observations to models to assess if current simulations of Sahelian boundary layers are accurate, and if not, what impact this could have on other aspects of model representation over West Africa such as moisture fluxes.

The European Centre for Medium Range Weather Forecasting (ECMWF) model and the UK Met Office Unified Model (UM, Cullen 1993) are used in section 4 for comparisons to observations. The performance of these models is of interest, as both are used operationally and widely within the research community. Using two gives a reference to each of them, to ascertain whether features are repeated in an alternative model.

The ECMWF analysis, version $T_L511L60$ is used with a resolution of approximately 40 km with 60 levels in the vertical (documentation available from www.ecmwf.int/publications). The Met Office UM operational global forecast model, version 6.1, has been run in place of using the analysis because of its flexibility of output time and choice of parameter output. The resolution of the model is approximately 40 km meridionally, 60 km zonally at 15°N, with 50 vertical levels. The UM forecasts are initialized from the UM analysis at 0000 UTC on the day of each case study, hence comparisons at 1800 are with the 18 hour UM forecast and at 0600 are with the 30 hour UM forecast.

c. Overview of the season

The 2005 summer monsoon season produced above-average rainfall across most of the Sahel compared to the climatology of 1979 - 2000 (Shein 2006). This climatology does not take into account the negative trend in Sahelian rainfall over the last 100 years, which, contrary to the above, suggests 2005 was a below-average year for rainfall.

The ECMWF analysis was used to document the synoptic situation in which the observations were taken, in order to evaluate possible larger scale influences. AEW troughs were tracked using the technique outlined in Fink and Reiner (2003), where 2-6 day filtered

meridional winds and relative vorticity above a threshold of 10^{-6} s^{-1} were used to identify the position of the northern and southern troughs. The troughs were initially identified by a hovmoeller plot, and manually tracked every 6 hours from the wind and vorticity plots.

The analysis suggested that seven AEWs crossed West Africa during August 2005, which was also a particularly active period of hurricane activity in the Atlantic. During the ballooning period, four AEW troughs moved across, reaching the field site longitude on approximately 7, 12, 17 and 21 August.

3. General results and generic observations of the NBL

Data were collected on twelve nights in August 2005, summarized in Table 1. Four full nights' worth of data were collected from 1800 UTC to approximately 0600 UTC. When a night's data is referred to, it will be given the date at the beginning of the night's experiments, so for example the night of the 12 August will also include the morning of 13 August.

Physical processes in NBLs are non-linear and the information from table 1 demonstrates that atmospheric conditions vary from night to night. However, there are some common features which typify the NBL. In this section, we present a composite of many of the experiments from different nights to describe the common features of the Agoufou NBL.

The profiles from ten nights (9, 11, 12, 13, 14, 15, 17, 18, 20, and 21 August) were gathered together to present composite plots of the changes in wind, potential temperature and humidity overnight in the lower boundary layer. The nights selected were used for their quality and quantity of observations. The profile altitudes were normalised against the boundary layer height for each night to reduce the impact of night-to-night variability

in boundary layer vertical structure. The normalisation presented some challenge, as the majority of profiles were available in the evening transition period between 1800 and 2300, hence boundary layer height, which is often defined by Richardson number (Garratt 1994; Mahrt et al. 1979) was noisy due to the breakdown of the daytime boundary layer and the setting up of the NBL. An alternative method of finding the boundary layer height was used from Vogelezang and Holtslag (1996).

In Vogelezang and Holtslag (1996) it was stated that boundary layer height, h, can be estimated from

$$h \equiv c\frac{u_*}{N} \tag{1}$$

where u_* is friction velocity, c is a constant and N is Brunt Vaisala frequency. Friction velocity was obtained from the Agoufou CEH flux station, available every 30 minutes. The constant c = 12, which assumes a non-neutral boundary layer (Vogelezang and Holtslag 1996). Different values of c were tested and found to make little difference to the overall structures observed in the final composite, however it should be noted that this value was calculated for the Cabauw site in the Netherlands and the validity in Agoufou has not been verified. The Brunt Vaisala frequency, N was found by

$$N^2 = (g/\theta_s)(\theta_h - \theta_s)/h. \tag{2}$$

Here θ_s and θ_h are potential temperatures at the surface and at height h, and g is acceleration due to gravity. Potential temperature was used rather than virtual potential temperature due to missing humidity data on some nights significantly reducing the number

of points available for averaging. Using equations (1) and (2), the height of the boundary layer was found when h and the sampled height, z, converge on the same value.

Boundary layer height alters throughout the night and is very low immediately after sunset when the day time layer is breaking up and the NBL is not established. For this analysis, boundary layer heights which decreased with time were rejected in favour of growing layers. A linear fit was applied to the values of boundary layer height for each night so that h was varying in time. Values in the fit below 15 m were rejected and set to 15 m, and values in the fit above the maximum measured boundary layer height were set to this maximum value. To normalize different nights boundary layer height by a reference value, an Agoufou 'average' boundary layer height which varied in time was created. A linear fit of all data points of boundary layer height was used as an approximation of average boundary layer height. Figure 1 shows the position of the boundary layer height each night, along with the fit for 'average' boundary layer. Again, the average boundary layer height was set so that values less than 15 m were rejected and set to 15 m, and values in the fit above the maximum boundary layer height were set to the maximum recorded value. A square root fit would be more ideal; however given the sparseness of data points, the linear fit is a reasonable first approximation.

The sampled altitudes were normalized by the night's boundary layer height, h_t, and the Agoufou 'average' boundary layer height, H_t, at each time, t, such that new altitude for the profiles was given by

$$H_t \frac{z}{h_t} \tag{3}$$

The values were loaded into a grid with 30 minute, 10 m boxes and values in each box were averaged. Figure 2 was produced, showing the time-normalised height plots for the various parameters using 146 profiles. The plots are smoothed using a three point running mean interpolation. A linear interpolation was also applied between gaps for presentation: approximately 25% of the plots are gap-filled. The result is a composite which shows the main signal from a combination of all nights.

For potential temperature and wind direction, differences from the mean values of the profiles before sunset (1830 UTC) were used. Using the differences removes the effect of each night's different initial conditions, and presents a clear evolution of the boundary layer overnight. When the same technique was used for the wind speed and mixing ratio, the signal was lost due to averaging and missing values near the beginning of the night, hence a simpler averaged plot of wind speed and mixing ratio from all profiles is shown.

It should also be noted that the composite uses information from fewer nights in the later part due to data availability (see table 1 for profile times), which may lead to some biasing of the signal after 0200. Despite this, figure 2 can still be used to distinguish structures which are common to the Agoufou NBL, and is a useful visualisation tool if used with these limitations in mind.

Potential Temperature

The observations revealed some consistent structures in the NBL evolution. On most of the nights the surface layers showed a defined inversion in temperature after sunset due to rapid cooling at the surface. This strong gradient was mixed upwards from the surface during

the night until it escaped the vertical range of the balloon. After that time the temperature throughout the sampled layer was more uniform. Throughout the night, the temperature at the surface continued to decrease, though in the cases where there were measurements further into the night, the nocturnal cooling rate decreased.

Mixing ratio

Mixing ratio was higher near the surface after sunset, and decreased rapidly with height above H(z/h) = 100 m. Later profiles showed a complex structure in the mixing ratio and figure 2(b) shows some moistening throughout the composite NBL between midnight and 0300 UTC.

It is possible that the increase in moisture in the composite is the signature of horizontal advection of moister air from lower latitudes due to the monsoon inflow Lothon et al. (e.g. 2008). It is also possible that some moistening is due to evaporation from the soil pores or directly from the plant canopy. The drying seen after 0330 was based on fewer profiles, but coincided with faster wind speeds and more mixing taking place in the early hours. A possible explanation is therefore that the available moisture was mixed higher throughout the boundary layer, resulting in a decrease in mixing ratio in the lower layers.

Wind speed and direction

During the night a stable nocturnal layer developed from the surface. The wind speeds above approximately H(z/h) = 100 m increased rapidly once the inversion was set up, due to the reduction in turbulence associated with a stably stratified profile. An increase in

wind speed was recorded for all nights, with a low level jet observed on several nights above H(z/h) = 150 m. The increase in speed between 150 and 200 m is consistent with similar observations from semi-arid regions (Lothon et al. 2008; Mahrt et al. 1979; Washington and Todd 2005), which have shown jet formation taking place between 200-400 m. The higher wind speeds eventually led to the erosion of the inversion from above through shear-driven mixing.

There were often only very weak changes in wind direction recorded by the tethersonde during the night, shown in figure 2(c), though some signal may be lost due to variability and averaging. The weak direction changes are in agreement with the Agoufou surface station data, where the August mean directional change from evening to morning was 40 degrees, and not consistently anticlockwise. Blackadar (1957), Buajitti and Blackadar (1957) and Thorpe and Guymer (1977) describe the inertial oscillation processes which lead to the turning of nocturnal jet winds with time. One full inertial oscillation at the location of Agoufou would take approximately 46 hours to complete due to the low latitude. This translates an expected change in wind direction of 90 degrees over the course of the night, therefore the observed wind changes were less than expected. This suggests that the inertial oscilliation is being damped, possibly by frictional forces or more dominant ageostrophic components (see conditions for inertial oscillation in Davis 2000) due to the low altitude of the measurements.

In general the direction of the wind maximum for each night was from the south-west. The direction of the prevailing monsoon wind at this latitude is from the south-west rather than from the south due to the Coriolis effect acting on synoptic scale wind motions and the presence of the heat low maximum over Algeria, Northern Niger and Northern Mali.

The wind observations showed that there were significant variations in strength from one night to the next. It often appeared in the data that on the nights where there was a stronger inversion, faster wind speeds were recorded by the balloon.

The relationship between inversion and jet strength will be explored in section 4 using the gradient Richardson number (Ri) to analyse the tethersonde data. A large Ri due to stable conditions and a strong inversion, would indicate a less turbulent atmosphere, suggesting any jet would be more free to accelerate. Therefore on nights where Ri is higher, the wind speed in the jet is expected to be faster. However, later in the night, a stronger jet would lead to more shear and more turbulence, reducing the value of Ri. Turbulence becomes more significant as Ri tends to 0.25 (Oke 1987), though this value may be higher, up to 1, for intermittent turbulence to occur (Mahrt 1999; Zilitinkevich and Baklanov 2002). Therefore the turbulence generated by the jet, coupled with a mixing and erosion of the inversion strength would lead to lower values of Ri later in the night. In contrast, nights when Ri values are low early on in the night, would be expected to retain relatively constant values throughout.

4. Case study nights

The profiles showed variability in observed features from one night to the next. Two case studies have been selected to highlight the variability and to discuss possible mechanisms which account for the differences. The 11 August and 18 August were chosen because of the variety in observed features between the two nights and for their quality of observations.

Table 2 presents data from the surface stations at Agoufou, Edgerit and Bamba to provide

a comparison to the balloon data and an evaluation of the main observed features. Wind direction for the start of the night is an average between 2000 and 2300 to reduce the impact of unsteady wind changes during the nocturnal transition phase immediately after sunset.

a. Night of 11 August 2005

a. Boundary layer observations

The day of 11 August was one of the hotter days of the experiment period. The temperature difference between day and night was large at all stations. A selection of five profiles from 11 August are shown in figure 3. Sixteen profiles were completed overall. The nocturnal profiles provide a classic 'textbook' example of the evolution of the NBL, where the temperature, humidity and wind direction profiles are all closely interlinked, such as in Garratt (1994).

Figures 3(a) and 3(d) show strong near-surface temperature and humidity inversions present immediately after sunset. During the night the temperature profile below 100 m became less stable as the wind speed increased, and temperature and humidity became more uniform throughout the layer.

The nocturnal jet formed at the top of the sampled layer, with wind speeds increasing steadily above 50 m throughout the night. The measured wind speed reached a maximum of 12 m s^{-1} at approximately 120 m above the ground at 0300 UTC (not shown). Wind direction was steadily from the south-west. The only notable large change in direction was close to the surface; however this can be accounted for by the lightness of the winds causing instability in the direction of the sonde.

The plot of gradient Richardson number, figure 3(c), shows high levels of stability (high Ri) higher up and a shallow layer near the surface where Ri was low. In general Ri decreased in time towards the end of the night, occurring at the same time as a decrease in the strength of the inversion, and an increase in wind shear with the increasing jet strength.

Table 2 shows some of the automatic weather station data for the night of 11 August. The winds exhibit similar speeds at all stations and reach their maximum at 2 m at similar times. The change in wind direction during the night is small at both Agoufou and Bamba, but larger at Edgerit. A closer inspection of data showed that the large swing at Edgerit occurred after 0300 UTC and before this the wind direction had changed very little. The change to more northerly flow at Edgerit occurred from 0400 to 0700 UTC and coincided with a period of very low wind speed (close to 1 m s^{-1}).

b. Comparisons with numerical models

The ECMWF operational analysis and the Met Office UM operational forecast model at global resolution were compared to the balloon data. The ECMWF operational analysis was available for only 1800, 0000 and 0600 UTC, so the observations as close as possible to these times were used in the comparisons.

Figure 4 shows that the observed wind direction agrees with models at 0008 and 0405 UTC, lending confidence to both models and observations as representative of large scale boundary layer flow later in the night. The discrepancies in the 1822 UTC profiles cannot be explained, but it is likely that the models are influenced by incorrect local flows or convection since they disagree with each other as well as the observations. Figure 4 also shows that the

ECMWF model depicts a weaker nocturnal jet at 0000 and 0600 UTC than was observed. Comparisons with the Met Office UM operational forecast model also showed that the wind speeds observed by the balloon were higher than those predicted by the UM forecast. The UM showed a consistent bias in temperature of approximately 2 K less than observations. The ECMWF also underestimated temperature, most notably at 0600.

c. Synoptic scale events - ahead of a trough

Wave tracking, using the technique explained in section 2c, showed an AEW trough located 500 km to the east of the fieldsite with the northern vortex centred at 20°N, 1°E at 00 UTC on 12 August. This was the second trough to pass during the experiment period.

The UM and ECMWF models both showed consistent south westerly winds in the boundary layer in line with the positioning of the trough and geostrophic balance. This lends confidence to the assertion that tethered balloon measurements reflected the larger scale wind direction for this night.

b. Night of 18 August 2005

a. Boundary layer observations

The balloon observations on 18 August are shown in figure 5. The temperatures were approximately 4°K cooler than on the 11 August, and the wind speed was less. The wind was particularly calm after sunset near the surface, and the sonde recorded < 1 ms^{-1} in the lowest 20 m in the 1909 sounding. This lack of wind only occurred on one other night,

15 August at 1923, when a storm was observed to the north at the same time. At sunset on 18 August, sporadic cumulus congestus with rain shafts were observed. It could be on both these days that outflows from storms acted to cancel the developing surface winds, or influenced the boundary layer decoupling from the land surface. It would be a point for further investigation to assess whether this is a common condition in Sahelian boundary layers, and a motivation for more nocturnal boundary layer observations.

The balloon observations displayed a bimodal wind direction on 18 August which was not observed on other nights. Figure 5 shows the rapid change in wind direction between the 0002 UTC profile and the 0207 UTC profile. Before midnight the wind direction recorded by the tethersonde was predominantly from the south-east. This changed abruptly at midnight to a more south-westerly direction. Agoufou station data for the night (table 2) showed a light south-westerly flow near sunset changing to a south-easterly direction by 2200 UTC. A rapid change back to the south-west was also seen in the station data at midnight. The same directional change from south-easterly (mean 2000 to 2300 UTC) to south-westerly winds (mean 0300 to 0600 UTC) was seen in the station data at Edgerit and Bamba. The corresponding wind speed was also recorded as being extremely low at all stations.

The wind change at midnight was not associated with a gust front, as no notable changes in temperature (nor humidity) were recorded in the station or balloon data. However the sonic anemometer at Agoufou measured a short burst of high turbulent kinetic energy at the same time as the wind change to south-westerly. The ground measurements, coupled with the balloon data, indicate that there was possibly some mesoscale circulation influencing the region, with wind from the east which developed against a weak monsoon inflow from the south-west. The burst in turbulence could have indicated the arrival of a convergence line

and therefore a change of the dominant influence on boundary layer winds.

Thus, the balloon data depicted an uncertain balance between two flows during the first part of the night, which was resolved by station data at the model grid scale (50 to 200 km). The second part of the night was more homogeneous in terms of wind direction.

The wind speed recorded by the tethersonde did not increase significantly during the night, unlike most other nights, and speed was seen to decrease somewhat in the later profiles. In comparison to the profiles taken on 11 August and the average profile of figure 2, the temperature and humidity inversions on 18 August were less pronounced. The Ri plots show a much higher level of turbulence (lower Ri) throughout the profile than on 11 August. This is in line with the observation in section 3 that low stability and low jet speeds are interlinked. This is also linked to radiative cooling as more cooling would lead to higher stability and faster jets, as seen in the observations at the Cabauw tower of Baas et al. (2009). The sensible heat flux at Agoufou, shown in table 2, demonstrates that the 18 August had less cooling at night than the 11 August, confirming that the 18 August satisfied these conditions likely to cause slower wind speeds near the surface.

b. Comparisons with numerical models

Figure 6 displays comparisons between the balloon observations, the ECMWF analysis and the UM forecast. Both models simulated changes in wind direction during the night, from south-east to south-west. In general models will be expected to show better skill at simulating large scale air motions. Their qualitative agreement with the balloon observations could indicate that wind direction was influenced by mesoscale or large scale wind patterns

rather than isolated local effects or convective outflow at Agoufou.

As for 11 August, the ECMWF model tended to underestimate wind speed. The UM wind speed was similar to observations at 0000 UTC and underestimated at 0600 UTC. Temperatures in both models were mainly cooler than observations.

c. Synoptic scale events - behind a trough

Wave tracking found an AEW trough axis located to the west of the field site on 18 August. This was the third wave event during the experimental period. Figure 7 shows the corresponding positions of vorticity maxima and UM winds at 925 hPa at 0000 UTC on 19 August 2005; the northern centre of the AEW is notably to the west of the southern centre.

In the early evening, UM boundary layer winds at 925hPa were from the south-east, reflecting the influence of the synoptic trough. Later model analysis showed a switch to more south-westerly winds, and a strengthening of the nocturnal jet as geostrophic wind associated with the surface heat low and monsoon inflow reached the site location. By 0600 UTC a strong south-westerly flow existed over Burkina Faso, southern Mali and Niger associated with the low level monsoon. The UM simulated a gradual change in wind direction unlike the sharp change in direction at midnight observed by the tethersonde and surface stations. The switch in winds to the southwest during the night did not occur in the model 850 hPa winds, and the mid-troposphere winds continued to be south-south-easterly.

This case has displayed wind directional changes which were consistent between surface stations, the balloon data and model and are explained by the large scale synoptic situation. This could indicate that the local boundary layer can be affected by trough passage if

conditions are favourable.

5. Discussion

The results from the tethered balloon experiments and the subsequent investigations with numerical models have provided new information on the boundary layer evolution in the Sahelian region of West Africa. The direction and speed of the winds observed by the balloon on all nights is consistent with the expected monsoon flow shown in the analysis of dropsondes in (Parker et al. 2005b). The rate of change at which the wind speed increases on some nights suggests a fast switching mechanism between convective vertical circulation domination and monsoonal, horizontal influences.

For both case studies detailed, the maximum nocturnal wind speeds were underrepresented in the two global models used for comparison. This in contradiction to Cuxart et al. (2006), where comparisons between several global models and a Large-Eddy Model showed overestimation of mixing and near-surface friction velocity by operational models. However, our findings are consistent with the modeling studies of the Bodélé NBL in Todd et al. (2008), where there was an underestimation of the observed jet by models. Agusti-Panareda et al. (2009) looked at mean ECMWF model biases in comparison to radiosonde data and found systematic errors in temperature in the Sahel region and a general overestimation of winds in contradiction to our findings from the case studies. However, the diurnal cycle, and the NBL was not isolated in the study so it may be that boundary layer mixing is too high at night, but the day time positive bias in wind dominates the mean signal. Since the southerly, nocturnal winds are primarily responsible for the northwards transport of mois-

ture, it is important to investigate how an underestimate of low level wind strength affects the moisture flux.

Figure 8 shows profiles of night time horizontal moisture flux from observations and UM simulations for the nights of the case studies using time-averaged profiles from each of the times presented in figures 4 and 6. The graphs show wind speeds multiplied by specific humidity and density for each level recorded. For 11 August, there is a much greater mean moisture flux from observations than model for the night. When the fluxes were integrated over 12 hours over a depth of 130 m, the mean flux from the observations was 0.11 kg m^{-2} s^{-1}, compared to 0.07 kg m^{-2} s^{-1} in the model. The model underestimates the moisture flux in this layer, which is expected as the winds were significantly underestimated for the night. For 18 August however, the model mean moisture flux over 60 m for the night was 0.06 kg m^{-2} s^{-1}, closer to the observations integrated over the same depth, 0.04 kg^{-2} s^{-1}. This was due to the overestimation of moisture by the model in the earliest profile. This compensates for the lower winds, achieving a good representation of the overall moisture flux on the nights where the model predicts high specific humidity.

To assess the significance of moisture transport in the lower layers, radiosonde profiles from Niamey (13.48°N, 2.17°E) for July and August 2006 were examined and the result from August is shown in figure 9. Both months' data showed that the moisture transport northwards primarily takes place in the lower layers, below 900 hPa in agreement with Lothon et al. (2008). This level was often reached in the balloon measurements, indicating that the findings of this study have wider implications for moisture transport.

Despite the underestimation of winds by the models, it should be noted that there have been changes to the boundary layer schemes in more recent versions of both the UM (version

6.3, Brown et al. 1957) and the ECMWF (Tompkins et al. 2004), since the versions of the models used in this study. It would be beneficial in future work to revisit observations in the Sahel region to establish whether the deficiencies still exist using these schemes. Our results emphasise the need for accurate depiction of the speed of winds in the boundary layer, and show how underestimation has consequences for moisture flux estimation which could in turn impact on convection prediction.

Returning to the balloon observations, local nocturnal boundary winds generally aligned with south westerly flow into the continent-scale heat low. However, there was evidence that winds could be influenced by changes in mesoscale or synoptic scale flow. The times when wind direction appeared to be influenced by larger scale movements (as on 18 August), were when wind speeds were lower, at times when there was a weaker monsoon inflow and therefore larger scale AEW dynamics could hold greater influence on boundary layer winds. This point requires further investigation as the evidence is taken from one case study only.

6. Summary and final comments

This is the first presentation of dynamical and thermodynamical observations taken of the nocturnal boundary layer of the climate sensitive Sahel region during the monsoon. These results have given some insight into real boundary layer features in a region which is very sensitive to changes in moisture and is particularly vulnerable to inter-annual variability of rainfall. Processes were observed to change at a very fine temporal scale; these would not be captured with 6 hour sampling and only marginally with 3 hour. Thus this data set is particularly useful for its time-resolution, and also for its abundance of surface station data

available to corroborate findings.

The observations have provided some confirmations of boundary layer structure theory and of numerical modeling. Strong inversions of temperature and humidity occurred directly after sunset. Inversions were eroded during the night by mixing caused by increases in wind speed and turbulence.

Due to the low altitude of the measurements, little turning of the winds was found and wind direction was generally observed to settle to the south-west by the early hours of the morning, despite any initial variation in direction. Comparisons with numerical models showed that observed wind speeds were higher than model wind speed and this could lead to an underestimation of moisture flux.

Correlations between unusual model and observed wind direction changes on 18 August 2005 suggested that the local boundary layer could be affected by non-local conditions on the large scale such as AEW activity.

Finally, the variability in these findings points to the need for more investigation into nocturnal boundary layers in this region. The role of nocturnal fluxes in synoptic dynamics is unknown and the link between boundary layer conditions and changes in convection and the alteration of synoptic features such as African Easterly Waves is yet to be explored.

Acknowledgments.

The authors would like to acknowledge the AMMA community and the people of Hombori and Agoufou for their support of this research. We would also like to thank Yakouba Traore and Frederic Baup for their help with operating the balloon and kite. We are grateful to Eric

Mougin and Franck Timouk at IRD in Mali for their support in organization. Thanks to Andreas Fink and Volker Ermet at the University of Cologne for providing the programs and support for wave tracking and to Anna Agusti-Panareda for information on the ECMWF model. UM modeling support was provided by NCAS and ECMWF operational analysis was obtained from the British Atmospheric Data Centre. Thank you to three anonymous reviewers whose comments improved the manuscript considerably. This work was supported by AMMA-UK and conducted as part of NERC PhD project NER/S/A/2004/12332.

Based on a French initiative, AMMA was built by an international scientific group and is currently funded by a large number of agencies, especially from France, UK, US and Africa. It has been the beneficiary of a major financial contribution from the European Community's Sixth Framework Research Programme. Detailed information on scientific coordination and funding is available on the AMMA International web site http://www.amma-international.org

REFERENCES

Abdou, K., D. J. Parker, B. Brooks, N. Kalthoff, and T. Lebel, 2009: The diurnal cycle of lower boundary-layer wind in the West African monsoon. *Quart. J. Roy. Meteor. Soc.*

Agusti-Panareda, A., A. Beljaars, C. Cardinali, I. Genkova, and C. Thorncroft, 2009: Impact of assimilating AMMA soundings on ECMWF analyses and forecasts. *ECMWF Technical Memoranda*, **601**.

Baas, P., F. C. Bosveld, H. K. Baltink, and A. A. M. Holtslag, 2009: A climatology of nocturnal low-level jets at Cabauw. *J. Appl. Meteor. Climatol.*, **48**, 1627–1642.

Berry, G. J. and C. Thorncroft, 2005: Case study of an intense African Easterly Wave. *Mon. Wea. Rev.*, **133**, 752–766.

Blackadar, A. K., 1957: Boundary layer maxima and their significance for the growth of nocturnal inversions. *Bull. Amer. Meteor. Soc.*, **38**, 283–290.

Brown, A. R., R. J. Beare, J. M. Edwards, A. P. Lock, S. J. Keogh, S. F. Milton, and D. N. Walters, 1957: Upgrades to the boundary-layer scheme in the Met Office numerical weather prediction model. *Bull. Amer. Meteor. Soc.*, **38**, 283–290.

Buajitti, K. and A. K. Blackadar, 1957: Theoretical studies of diurnal wind-structure variations in the planetary boundary layer. *Quart. J. Roy. Meteor. Soc.*, **83 (358)**, 486–500.

Burpee, R. W., 1972: The origin and structure of easterly waves in the lower troposphere of North Africa. *J. Atmos. Sci.*, **29**, 77–90.

Culf, A. D., 1992: An application of simple models to Sahelian convective boundary-layer growth. *Bound.-Layer Meteor.*, **58**, 1–18.

Cullen, M. J. P., 1993: The unified forecast/climate model. *Meteor. Mag.*, **122**, 81–93.

Cuxart, J., et al., 2006: Single-column model intercomparison for a stably stratified atmospheric boundary layer. *Bound.-Layer Meteor.*, **118**, 273.

Davis, P. A., 2000: Development and mechanisms of the nocturnal jet. *Meteor. Appl.*, **7**, 239–246.

Dolman, A. J., A. D. Culf, and P. Bessemoulin, 1997: Observations of boundary layer development during the HAPEX-Sahel intensive observation period. *J. Hydrol.*, **188-189**, 998–1016.

Fink, A. and A. Reiner, 2003: Spatio-temporal variability of the relation between African Easterly Waves and West African squall lines in 1998 and 1999. *J. Geophys. Res.*, **108**, 4332.

Garratt, J. R., 1994: *The atmospheric boundary layer*. Cambridge University Press, 340 pp.

Guichard, F., L. Kergoat, E. Mougin, F. Timouk, F. Baup, P. Hiernaux, and F. Lavenu, 2009: Surface thermodynamics and radiative budget in the Sahelian Gourma: Seasonal and diurnal cycles. *J. Hydrol.*, **375**, p161–177.

Hamilton, R. A. and J. W. Archbold, 1945: Meteorology of Nigeria and adjacent territory. *Quart. J. Roy. Meteor. Soc.*, 231–265.

Lebel, T., et al., 2009: The AMMA field campaigns: multiscale and multidisciplinary observations in the West African region. *Quart. J. Roy. Meteor. Soc.*

Lothon, M., F. Saïd, F. Lohou, and B. Campistron, 2008: Observation of the diurnal cycle in the low troposphere of West Africa. *Mon. Wea. Rev.*, **136**, 3477–3500.

Mahrt, L., 1999: Stratified atmospheric boundary layers. *Bound.-Layer Meteor.*, **90**, 375–396.

Mahrt, L., R. C. Heald, D. H. Lenschow, B. B. Stankov, and I. B. Troen, 1979: An observational study of the structure of the nocturnal boundary layer. *Bound.-Layer Meteor.*, **17**, 247–264.

McGarry, M. M. and R. J. Reed, 1978: Diurnal variations in convective activity and precipitation during phases I and II of GATE. *Mon. Wea. Rev.*, **106**, 101–113.

Mougin, E., P. Hiernaux, L. Kergoat, and et. al., 2009: The AMMA-CATCH Gourma observatory site in Mali: Relating climatic variations to changes in vegetation, surface hydrology, fluxes and natural resources. *J. Hydrol.*, **375**, 14–33.

Oke, T., 1987: *Boundary Layer Climates*. Methuan, London, 372 pp.

Parker, D. J., R. R. Burton, A. Diongue-Niang, R. J. Ellis, M. Felton, C. D. Thorncroft, P. Bessemoulin, and A. M. Tompkins, 2005a: The diurnal cycle of the West African monsoon circulation. *Quart. J. Roy. Meteor. Soc.*, **131 (611)**, 2839–2860.

Parker, D. J., C. D. Thorncroft, R. R. Burton, and A. Diongue-Niang, 2005b: Analysis of the African Easterly Jet, using aircraft observations from the JET2000 experiment. *Quart. J. Roy. Meteor. Soc.*, **131 (608)**, 1461–1482 Part B.

Pospichal, B., D. B. Karam, S. Crewell, C. Flamant, A. Hunerbein, O. Bock, and F. Said, 2009: Diurnal cycle of the intertropical discontinuity over west africa analysed by remote sensing and mesoscale modelling. *Quart. J. Roy. Meteor. Soc.*

Redelsperger, J. L., C. D. Thorncroft, A. Diedhiou, T. Lebel, D. J. Parker, and J. Polcher, 2007: African Monsoon Multidisciplinary Analysis - An international research project and field campaign. *Bull. Amer. Meteor. Soc.*, **12 (87)**, 1739+.

Shein, K. A., 2006: State of the climate in 2005. *Bull. Amer. Meteor. Soc.*, **87 (6)**, s1–s102.

Sultan, B. and S. Janicot, 2003: The West African Monsoon dynamics. Part I: Documentation of intraseasonal variability. *J. Climate*, **16**, 3389–3406.

Thorncroft, C. D. and B. J. Hoskins, 1994: An idealized study of African Easterly Waves. I: A linear view. *Quart. J. Roy. Meteor. Soc.*, **120**, 953–982.

Thorpe, A. J. and T. H. Guymer, 1977: The nocturnal jet. *Quart. J. Roy. Meteor. Soc.*, **103**, 633–653.

Todd, M. C., R. Washington, S. Raghavan, G. Lizcano, and P. Knippertz, 2008: Regional model simulations of the Bodélé low-level jet of Northern Chad during the Bodélé Dust Experiment (BoDEx 2005). *J. Climate*, **21**, 995–1012.

Tompkins, A. M., P. Bechtold, A. Beljaars, A. Benedetti, M. J. S. Cheinet, M. Kohler,

P. Lopez, and J.-J. Morcrette, 2004: Moist physical processes in the IFS: Progress and plans. *ECMWF Technical Memoranda*, **452**.

Vilà-Guerau de Arellano, J., 2007: Role of nocturnal turbulence and advection in the formation of shallow cumulus over land. *Quart. J. Roy. Meteor. Soc.*, **133**, 1615–1627.

Vogelezang, D. H. P. and A. A. M. Holtslag, 1996: Evaluation and model impacts of alternative boundary-layer height formulations. *Bound.-Layer Meteor.*, **81**, 245–269.

Wallace, J. S., J. H. C. Gash, and M. V. K. Sivakumar, 1990: Preliminary measurements of net radiation and evaporation over bare soil and fallow bushlan in the Sahel. *Int. J. Climatol.*, **10**, 203–210.

Washington, R. and M. C. Todd, 2005: Atmospheric controls on mineral dust emission from the Bodele Depression, Chad: The role of the low level jet. *Geophys. Res. Lett.*, **32**, L17 701.

Washington, R., M. C. Todd, S. Engelstaedter, S. Mbainayel, and F. Mitchell, 2006a: Dust and the low-level circulation over the Bodele Depression, Chad: Observations from the BoDEx 2005. *J. Geophys. Res.*, **111**, D03 201.

Washington, R., et al., 2006b: African climate change. *J. Geophys. Res.*, **111**, D03 201.

Zilitinkevich, S. S. and A. Baklanov, 2002: Calculation of the height of the stable boundary layer in practical applications. *Bound.-Layer Meteor.*, **105**, 389–409.

List of Tables

TABLE 1. *Summary of balloon/kite data fo nights in August 2005. Number of profiles (No. profs) is number of complete (up and down is one) profiles recorded. Time given in UTC; Wind speed given in m s^{-1}; Height given in m; Potential temperature in K; Mixing ratio in g kg^{-1}. Nights where a kite was used instead of a balloon are marked with a star. Nights where a kite was used for some profiles (3/12 on 11 August at end of night, 2/10 on 15 August at beginning of night) are marked by two stars. Dashes indicate where data are not available or are possibly unreliable*

Night	No. Profs	Profile Times		Wind Max		Potential Temp		Mixing Ratio	
		First	Final	speed	height	Max T	Min T	Max	Min
6*	1	19:10	19:32	9.9	138	311.1	306.9	15.9	14.4
7*	1	17:01	17:11	10.3	36	310.7	310.4	16.4	15.3
9*	3	17:21	21:19	5.4	61	305.3	301.1	19.7	14.9
11**	8	18:19	04:28	12.4	115	309.0	301.9	21.2	12.4
12*	7	17:17	05:58	12.5	111	305.5	297.9	17.4	–
13*	2	17:16	20:00	11.1	150	307.1	302.7	17.0	14.6
14	4	17:27	00:08	9.2	81	307.1	301.2	17.1	14.5
15**	6	16:50	23:19	6.2	57	309.0	300.3	18.6	13.9
17	11	17:15	05:28	7.8	154	305.5	298.7	–	–
18	9	19:09	05:54	8.3	177	304.7	298.6	20.2	–
20	5	18:41	02:04	9.1	106	308.4	300.0	20.1	14.1
21	6	16:18	00:32	11.5	247	308.9	301.3	20.7	13.5

TABLE 2. *Agoufou, Edgerit and Bamba surface station data for the case study nights. Temperature is used instead of potential temperature due to the unavailability of pressure data at Bamba. The periods of the observations are 24 hours starting at 0600 on the date indicated and finishing at 0600 the following day. Day is defined as 0600 to 1800, night is 1800 to 0600 UTC.*

		Agoufou		Edgerit		Bamba	
		11 Aug	18 Aug	11 Aug	18 Aug	11 Aug	18 Aug
Max 2m wind night ($m\ s^{-1}$)	Speed	4.2	1.8	3.7	4.4	5.4	2.3
	Hour	0100	0400	1830	0200	0145	1830
Night wind direction (degrees)	Mean 2000 to 2300	287	236	230	183	253	156
	Mean 0300 to 0600	301	261	279	205	257	236
	Min dir/ time	271/2100	142/2130	216/2230	165/1800	232/0500	51/2315
	Max dir/ time	325/0500	314/2330	359/0600	219/0030	282/0345	330/2330
Temperature (K)	Day max	307	302	313	308	311	304
	Night min	298	295	306	304	302	300
Mean H ($W\ m^{-2}$)	Day	41	55	131	155	-	–
	Night	-18	-4	3	2	-	–

List of Figures

9 Composite moisture flux $\mathbf{V}.q.\rho$ from all radiosonde profiles from Niamey for August 2006. Soundings at 12 UTC are represented by the thin/grey line, 18 UTC are bold/grey, 00 UTC are thin/black and 06 UTC are bold/black lines. Shading represents +/- standard deviation. 45

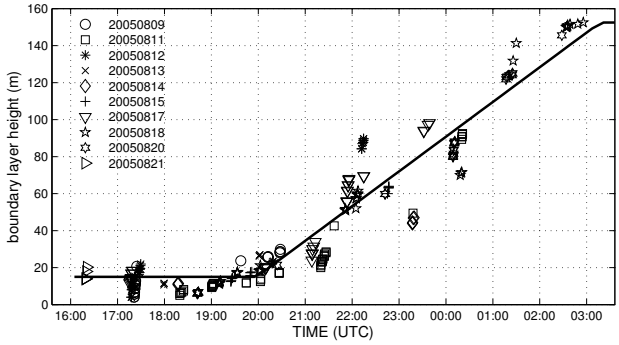

FIG. 1. Estimations of boundary layer height against time for different nights. The line represents the Agoufou average boundary layer height calculated as a fit to the data points available. This data is used to normalize heights of profile measurements so they may be used in the composite of figure 2.

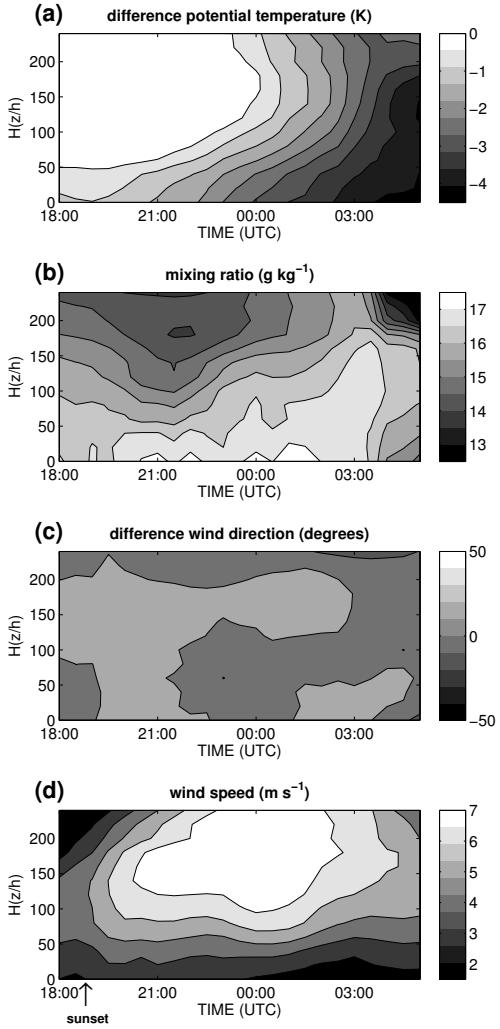

FIG. 2. Time against normalised height plots of (a) potential temperature, (b) mixing ratio, (c) wind direction and (d) wind speed composed from ten nights' worth of tethered balloon and kite profiles (dates in August 2005: 9, 11, 12, 13, 14, 15, 17, 18, 20, 21). The potential temperature and wind direction plots represent an interpolation of differences from initial values of parameters for all of the results collected from ten nights. The mixing ratio and wind speed plots show an interpolation of values from all of the results collected from nine nights.

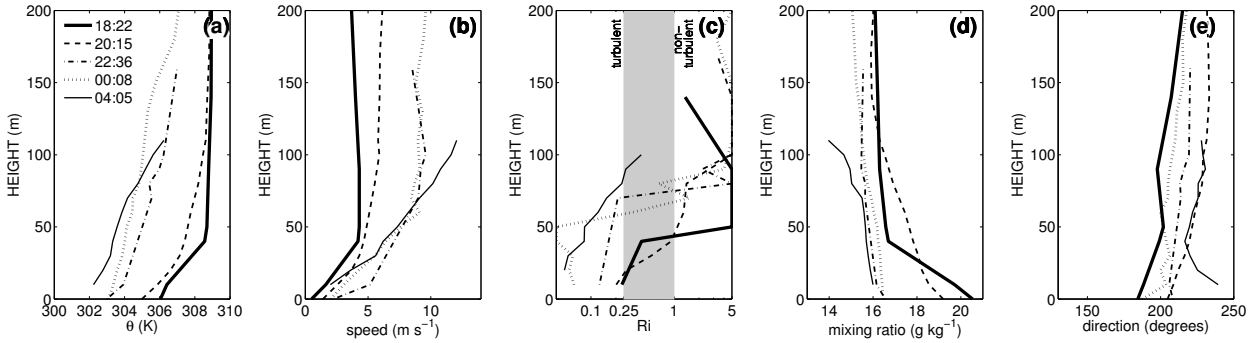

FIG. 3. Selected profiles from the night of 11 August 2005 at five times during the night: (a) potential temperature, (b) wind speed, (c) Richardson number, (d) mixing ratio and (e) wind direction. Times marked in the legend of panel (a). In (c) a line marks the transition at a value of $0.25<\mathrm{Ri}<1$ between stable and turbulent flow.

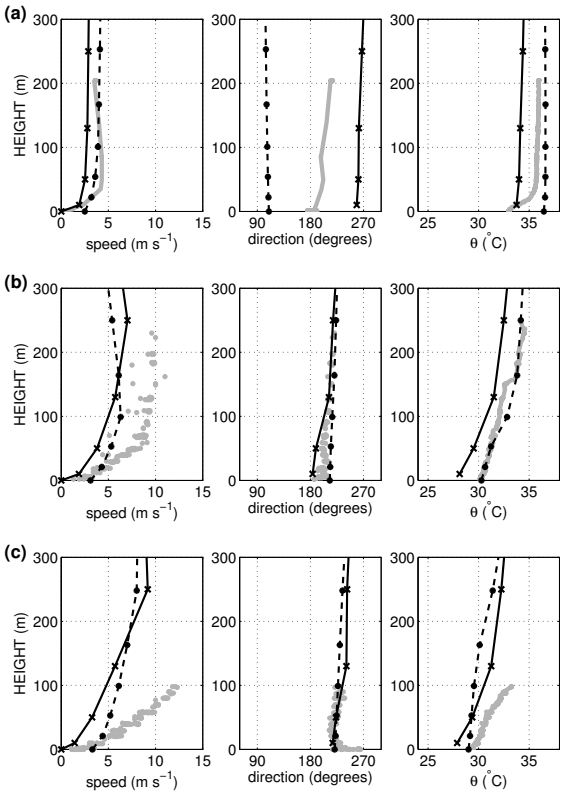

FIG. 4. 11 August 2005: Comparisons between the UM forecast (solid black line), ECMWF analysis (dashed line) and observations (grey line). (a) 1822 UTC Observations against UM and ECMWF at 1800 UTC, (b) 0008 UTC Observations against UM and ECMWF at 0000 UTC, (c) 0405 UTC Observations against UM at 0400 UTC and ECMWF at 0600 UTC.

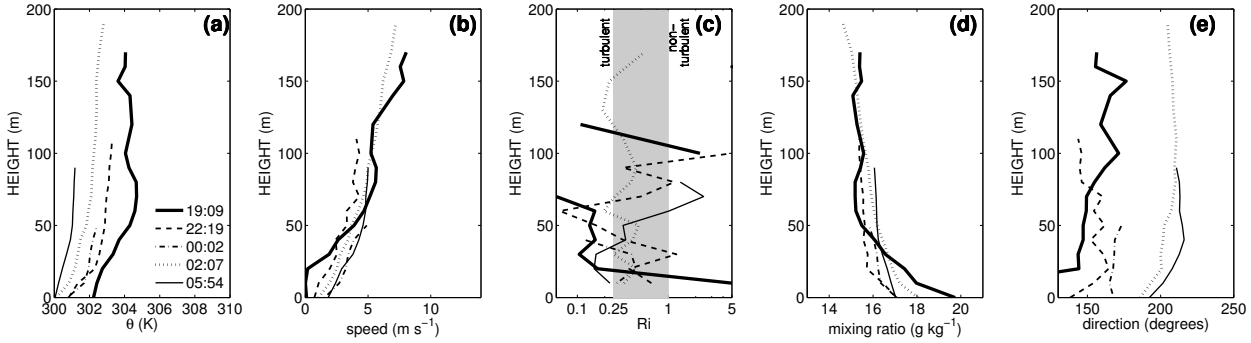

FIG. 5. As for Figure 3. Selected profiles from the night of 18 August 2005 at five times during the night: (a) potential temperature, (b) wind speed, (c) Richardson number, (d) mixing ratio and (d) wind direction. Times marked in the legend of panel (a).

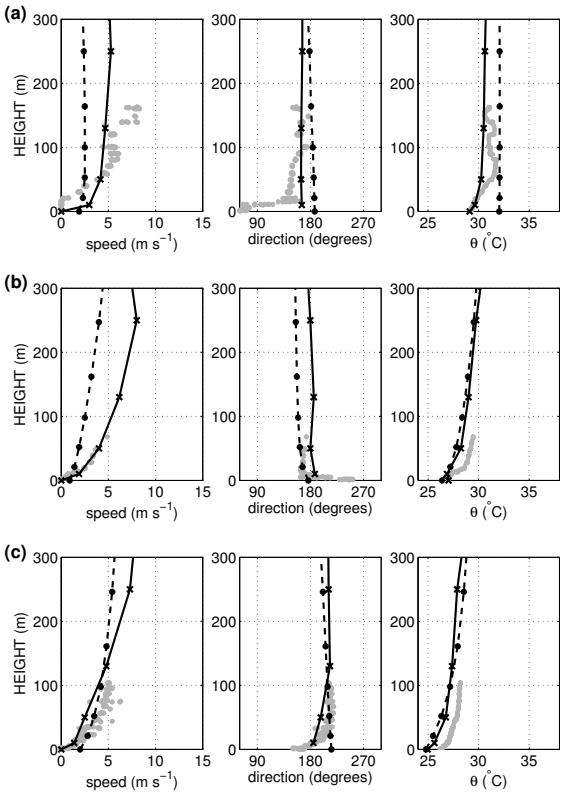

FIG. 6. 18 August 2005: Comparisons between the UM forecast (solid black line), ECMWF analysis (dashed line) and observations (grey line). (a) 1908 UTC Observations against UM at 1900 UTC, ECMWF at 18 UTC (b) 0002 UTC Observations against UM and ECMWF at 0000 UTC, (c) 0554 UTC Observations against UM and ECMWF at 0600 UTC.

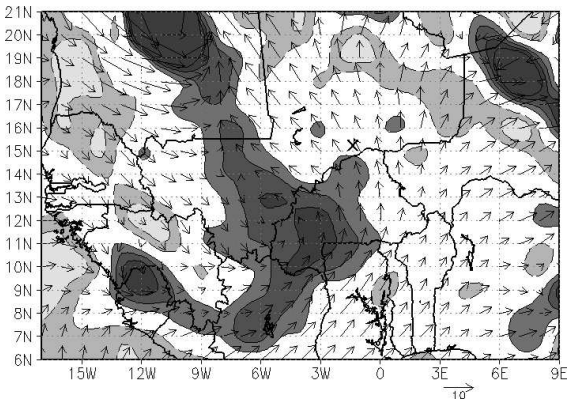

FIG. 7. Vorticity and winds from the ECMWF operational analysis at 925 hPa at 00 UTC on 19 August 2005. Positive vorticity is shown in black, negative in dashed light grey, while contours are every 10^{-5} s^{-1}. The field site is marked with a cross. A trough with two centers, north and south, can be seen to the east of Mauritania, west of Mali/ Burkina Faso.

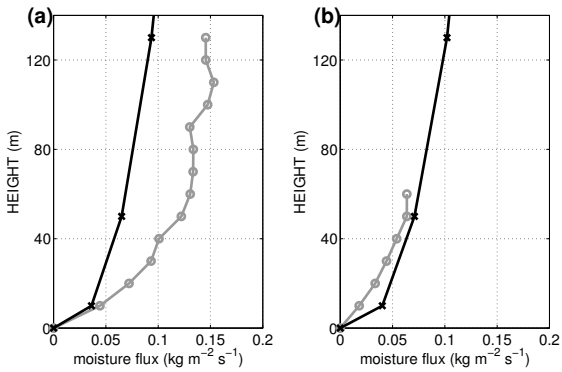

FIG. 8. Mean night time moisture flux ($\mathbf{V}$.q.ρ) comparisons in kg m^{-2} s^{-1}, from the evenings of 11 (a) and 18 (b) August 2005: observations in grey and UM in black.

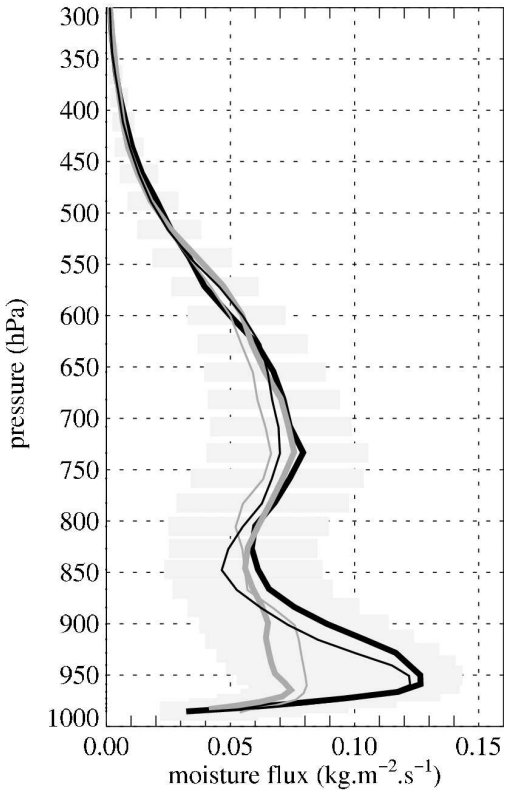

FIG. 9. Composite moisture flux $\mathbf{V}.q.\rho$ from all radiosonde profiles from Niamey for August 2006. Soundings at 12 UTC are represented by the thin/grey line, 18 UTC are bold/grey, 00 UTC are thin/black and 06 UTC are bold/black lines. Shading represents +/- standard deviation.